The Astrophysical Journal Letters, 803:L7 (6pp), 2015 April 10 doi:10.1088/2041-8205/803/1/L7

RADIAL AND AZIMUTHAL OSCILLATIONS OF HALO CORONAL MASS EJECTIONS IN THE SUN

Harim Lee[1], Y.-J. Moon[1], and V. M. Nakariakov[1,2]
[1] School of Space Research, Kyung Hee University, Yongin 446-701, Korea; harim@khu.ac.kr, moonyj@khu.ac.kr, V.Nakariakov@warwick.ac.uk
[2] Centre for Fusion, Space & Astrophysics, Physics Department, University of Warwick, Coventry CV4 7AL, UK
Received 2015 February 25; accepted 2015 March 20; published 2015 April 6

ABSTRACT

We present the first observational detection of radial and azimuthal oscillations in full halo coronal mass ejections (HCMEs). We analyze nine HCMEs well-observed by the Large Angle and Spectrometric Coronagraph (LASCO) from 2011 February to June. Using the LASCO C3 running difference images, we estimated the instantaneous apparent speeds of the HCMEs in different radial directions from the solar disk center. We find that the development of all these HCMEs is accompanied by quasi-periodic variations of the instantaneous radial velocity with the periods ranging from 24 to 48 minutes. The amplitudes of the instant speed variations reach about a half of the projected speeds. The amplitudes are found to anti-correlate with the periods and correlate with the HCME speed, indicating the nonlinear nature of the process. The oscillations have a clear azimuthal structure in the heliocentric polar coordinate system. The oscillations in seven events are found to be associated with distinct azimuthal wave modes with the azimuthal wave number $m = 1$ for six events and $m = 2$ for one event. The polarization of the oscillations in these seven HCMEs is broadly consistent with those of their position angles with the mean difference of 43°. The oscillations may be connected with natural oscillations of the plasmoids around a dynamical equilibrium, or self-oscillatory processes, e.g., the periodic shedding of Alfvénic vortices. Our results indicate the need for an advanced theory of oscillatory processes in coronal mass ejections.

Key words: Sun: coronal mass ejections (CMEs) – Sun: oscillations

1. INTRODUCTION

Coronal mass ejections (CMEs) are the most spectacular eruptions from the Sun into the heliosphere. They are usually the main sources of geomagnetic storms (Gosling et al. 1991; Gosling 1993). It has been found that the interplanetary propagation of CMEs is controlled by the ambient solar wind (Lindsay et al. 1999; Gopalswamy et al. 2000, 2001a, 2001b; Vršnak & Žic 2007). Several authors (Vršnak et al. 2004; Yashiro et al. 2004) suggested that the interaction between CMEs and the solar wind is an important mechanism that determines CME kinematics. One possible mechanism for the deflection of the CME trajectory from radial is the asymmetric aerodynamic drag force associated with the formation of Alfvénic Kelvin–Helmholtz vortices (Foullon et al. 2011).

Dynamical processes in the solar corona are often accompanied by the excitation of various kinds of oscillations of coronal plasma non-uniformities, with the periods ranging from a fraction of a second to several hours. The majority of coronal oscillations have been identified as MHD modes of the non-uniformities (see De Moortel & Nakariakov 2012; Liu & Ofman 2014, for recent comprehensive reviews). The interest in MHD oscillations is connected with a number of open questions, such as heating of the plasma, presence of additional sinks for the energy released in flares, triggering the energy releases, and MHD seismology—diagnostics of plasma parameters and physical processes operating in the plasma by means of MHD oscillations.

It is reasonable to expect that CMEs are accompanied by MHD oscillations that appear naturally as the response of the elastic and compressive plasma to the energy deposition. However, there have been a very few observations of oscillations associated with CMEs. Perhaps the first observation of CME oscillation was reported by Krall et al. (2001). Examining the evolution of the speed pattern of the leading-edge and trailing-edge features for a flux-rope-like CME, they found that the projected CME velocities varied with the period of about 4–6 hr. Shanmugaraju et al. (2010) developed that study, examining the speed–distance profiles of 116 CMEs with at least 10 height–time data points, and found that about fifteen CMEs had quasi-periodic oscillation patterns. In addition, they showed that the oscillation periods were within the range of the upper and lower limit of the Alfvén travel time along the magnetic rope of the CME. Very recently, a vertically polarized kink oscillation with the period of about 11 minutes was detected in a raising magnetic rope observed in EUV in the low corona (Kim et al. 2014).

In this Letter, we present the first detection of both radial and azimuthal oscillations in halo coronal mass ejections (HCMEs). This letter is organized as follows. In Section 2, we describe the data and analysis. Results are given in Section 3. A brief summary and discussion are presented in Section 4.

2. DATA AND ANALYSIS

We considered nine well-observed full HCMEs whose structures were clearly seen in the *Solar and Heliospheric Observatory* (*SOHO*) Large Angle and Spectrometric Coronagraph's (LASCO, Brueckner et al. 1995) C2 and C3 fields of view from 2011 February to June. These HCMEs were observed at heights from 4.0 to 27.3 $R_{\odot}$ with a cadence time of about 12–15 minutes. The dates, times, source locations and other properties of the events are summarized in Table 1. In the study we used running difference images obtained from the CDAW LASCO CME online catalog (http://cdaw.gsfc.nasa.gov/CME_list/). Figure 1 shows a typical event analyzed in this study, represented by three running difference images taken at different instants of time.

For each available running difference image of the HCMEs we estimated locations of the front edges of the HCME, the outermost and fastest moving structure, at the rays positioned at

Table 1
List of HCMEs with the Oscillation Parameters

Date	Time	Source Location	Measurement Position Angle	Duration	Distance	Projected Speed	Speed Amplitude	Period	Oscillation Direction	Wave Mode
(dd/mm)	(UT)		(deg)	(minutes)	($R_\odot$)	V_{pro} (km s^{-1})	(ΔV km s^{-1})	(minutes)	(deg)	($m = \#$)
2011 Feb 15	02:24:05	S02E12	279	60	5.4–16.7	800	400	24	75	1
2011 Mar 07	20:00:05	N24W60	43	48	5.2–27.3	2100	900	24	⋯	⋯
2011 Mar 21	02:24:05	N22W132	4	72	6.2–18.0	1300	700	24	⋯	⋯
2011 Apr 24	21:24:09	N20W175	166	96	4.0–12.1	600	200	48	30	1
2011 Jun 02	08:12:06	S19E25	188	120	4.8–19.0	800	300	48	135	1
2011 Jun 04	06:48:06	N15W150	14	48	4.3–21.0	1500	800	24	15, 105	2
2011 Jun 04	22:05:02	N15W160	30	74	5.2–23.6	1700	700	30	135	1
2011 Jun 07	06:49:12	S21W54	340	76	5.6–20.5	1600	700	30	60	1
2011 Jun 21	03:16:10	N39E01	155	144	5.7–13.6	600	400	48	120	1

Note. Column 1–2: the first appearance date and time of the HCMEs in the LASCO C2 field of view. Column 3–4: the source location and position angle reported in the CDAW LASCO CME catalog, respectively. Column 5–6: the duration of the observational interval and the distance range of the HCMEs. Column 7–8: the maximum projected speed (V_{pro}), and the maximum oscillation amplitude (ΔV). Column 9–11: the period, direction, and azimuthal mode number of the oscillation. If the field is blank, it means a rather complex wave pattern.

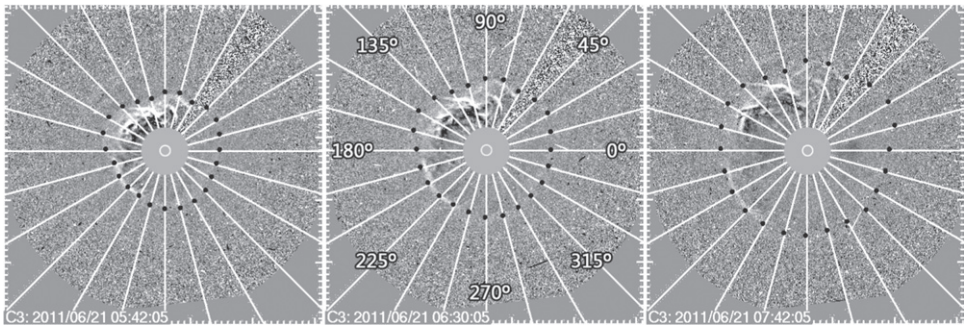

Figure 1. Running difference images of the propagation of the HCME on 2011 June 21 at 05:42–07:42 UT. The radial white lines show the rays taken every 15° from the west. The black dots show the front edge of the HCME. The white circles on the occulting disks mark the size of the Sun.

every 15° of the azimuthal angle defined as a counterclockwise from the solar west. These measurements were combined in the height–time maps constructed for different azimuthal angles. The instantaneous speed ($V_{\rm ins}$) of the HCMEs was determined using two successive height–time measurements at every azimuthal angle for at least four time intervals. Figure 2 shows that the instantaneous speed varies with time (height) quasi-periodically, rather than monotonically increases or decreases.

Parameters of the oscillations we determined by best-fitting the dependence of the instantaneous speed on time by the harmonic function $V_{\rm ins} = \Delta V\ \sin(\omega(t - K)) + b$, where ΔV is the amplitude, ω is the cyclic frequency, K is the phase, and b is the mean value, with the use of the least-square method. We also estimated the observed projected speeds ($V_{\rm pro}$) of the HCMEs at every azimuthal angle, which were obtained from a linear fit of height–time data. The results are shown in Table 1.

Some uncertainties in determining the speed of the HCMEs may exist because the determination of the HCME front edge locations are made by the visual inspection. To estimate the uncertainty of the instantaneous speed estimation, we made 10 independent trials of the measurements of the front edge locations. Then the error was calculated as its standard deviations for each HCMEs, and the mean value was taken as the measurement. In this study, we estimate the uncertainty of the speed measurement to be about 200 km s^{-1}, which is an average of the standard deviations. We find that the speed amplitudes ΔV in all the analyzed events.

Figure 2 shows the oscillatory patterns in the instantaneous speed variation are rather systematic, and have an obvious angular dependence. Several HCMEs (e.g., ♯1, 5, 9 in Table 1) originated from the solar disk center and produced full-halo CMEs with mostly circular shapes. For these cases, the oscillation patterns of these HCMEs at a certain azimuth angle approximately show radial oscillations. To quantify the azimuthal dependence of the oscillatory patterns, we consider the azimuthal dependence in the form of the harmonic function $\exp(im\ \theta)$, where θ is the azimuthal angle, and m is an integer representing the azimuthal wave number.

To determine the azimuthal wave number of the oscillations, we applied the following procedure: (1) according to the phase of the oscillations (see the left panels of Figure 2) we grouped the oscillations detected along individual rays corresponding to different azimuthal angles into "positive" and "negative"; these two groups are shown in the right panels of Figure 2 by the red and blue circles; (2) we positioned nodal lines between the "red" and "blue" rays; (3) the azimuthal mode number m of the oscillation was obtained as the number of the nodal lines. The polarization of the oscillation was determined in the direction that was perpendicular to the nodal line for $m = 1$, and 45° from the nodal line for $m = 2$. The white and black arrows show the directions of the oscillation polarization. The yellow arrows show the HCME position angles (obtained from the LASCO catalog). We found that the polarization directions are roughly consistent with the HCME position angles with the average discrepancy of 43°.

3. RESULTS

We estimated instantaneous radial speeds of nine full HCMEs at every 15° azimuthal angle along 24 rays altogether for each HCME. We found that all the HCMEs had oscillatory patterns in the instantaneous speeds. These oscillatory patterns were found to have opposite phases in different groups of azimuthal directions. As seen in the right panel of Figure 2, the oscillatory patterns were clearly presented in about 40% of the azimuthal angles. In the left panel of Figure 2 we give several typical examples of the oscillations. In particular, the 2001 February 15 event (Figure 2(a)) is a good example of the $m = 1$ mode. The observed maximum projected speed and the instantaneous speed oscillation amplitude were found to be about 800 and 400 km s^{-1}, respectively. The oscillation period of the HCME is about 24 minutes. The 2011 June 2 event (Figure 2(b)) is another case of the $m = 1$ mode. The observed maximum projected speed and the instantaneous speed amplitude are 800 and 300 km s^{-1}, respectively. The oscillation period of the HCME is about 48 minutes. The 2001 June 4 event (Figure 2(c)) is a good example of the $m = 2$ mode. The observed maximum projected speed and the speed amplitude are 1500 and 800 km s^{-1}, respectively. The oscillation period of the HCME is about 24 minutes. The 2001 March 21 event (Figure 2(d)) has a rather complex azimuthal pattern. The red and blue circles appear mixed (Figure 2, right panel). The observed maximum projected speed and the speed amplitude are 1300 and 700 km s^{-1}. The oscillation period of the HCME is about 24 minutes.

Figure 3 shows two examples of HCME speed profile ($V_{\rm ins(max)}$) with the maximum amplitude and their comparison with the harmonic functions. We find that the observed maximum speeds are approximately fitted by the harmonic functions. The oscillation parameters and the azimuthal mode numbers of all nine events are summarized in Table 1. Durations of the oscillations were found to range from 48 to 144 minutes. The oscillation period ranges from 24 to 48 minutes with the average of 33.3 minutes. In all the events except two the azimuthal wave patterns were found to belong

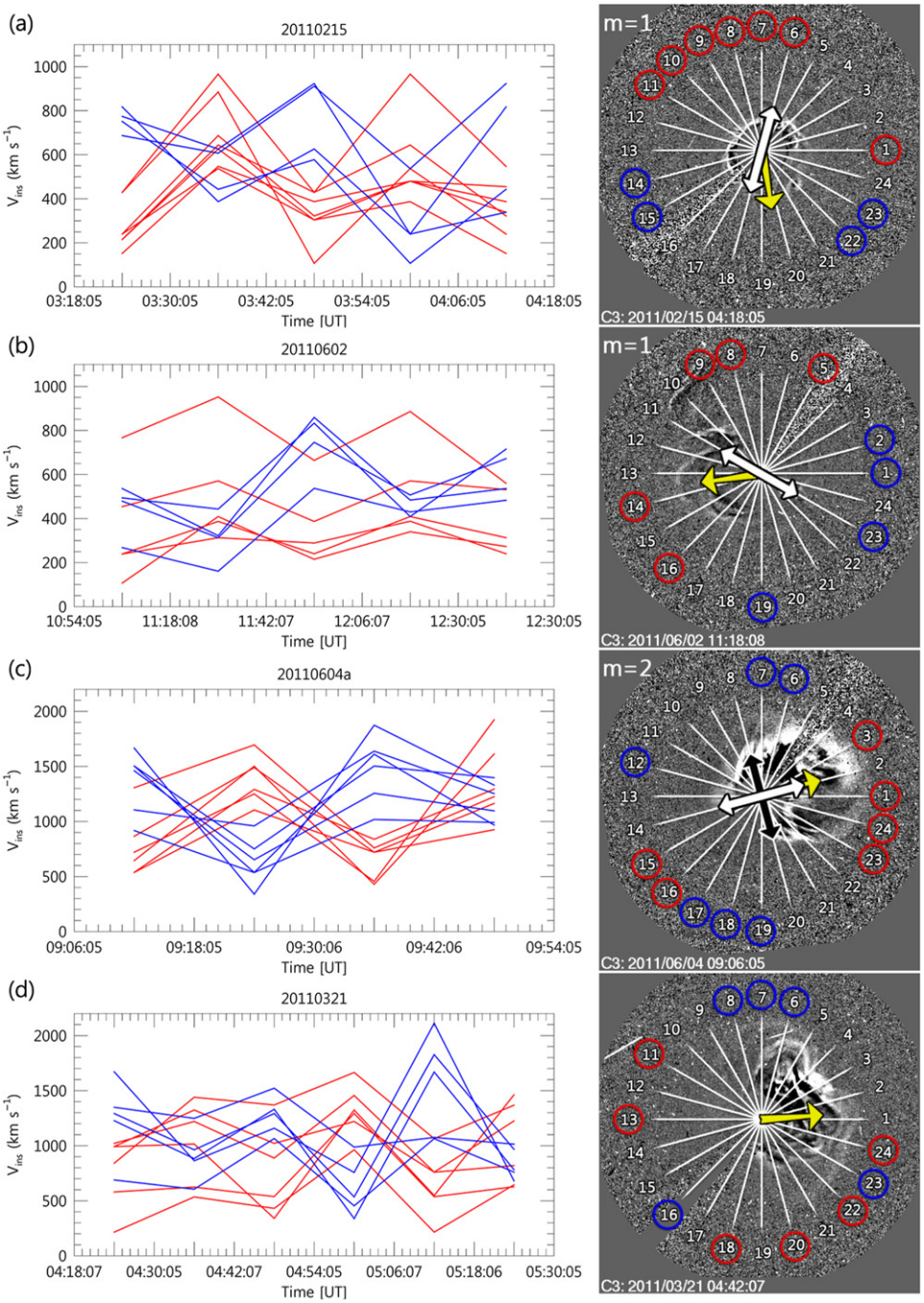

Figure 2. Left panel: the variation of the instantaneous speed of the HCME with time along different azimuthal rays. The red and blue colors correspond to two groups with different phases. Right panel: the azimuthal dependence of the oscillations. The white numbers enumerate the azimuthal rays. The red and blue circles indicate the oscillations of opposite phases. The white and black arrows show the directions of the oscillation polarization. The yellow arrows show the HCME position angles. In the left top corners the azimuthal mode numbers are indicated.

to two lowest azimuthal wave modes, $m = 1$ in six events and $m = 2$ in one event.

Figure 4(a) shows a relationship between the oscillation amplitude and maximum projected speed. We found that there is a good correlation, with the correlation coefficient of 0.92, between these two quantities. The speed amplitudes are about a half of the projected speed. Figure 4(b) shows a relationship between the speed amplitude and oscillation periods. It is found that the speed amplitude anti-correlates linearly with the period. The oscillation period is thus inversely proportional to the projected speed.

4. SUMMARY AND DISCUSSION

Our study demonstrates the periodic variation of the instantaneous projected radial speed of halo coronal mass ejections. In the lower solar corona, long-period oscillations, with the periods similar to discussed in this Letter, are often detected in prominences (e.g., Foullon et al. 2009; Bi et al. 2014). The oscillations are detected to be either excited by impulsive energy releases (e.g., Hershaw et al. 2011), or result from some over-stabilities processes (e.g., Tripathi et al. 2009). It is not clear whether the HCME oscillations belong to the

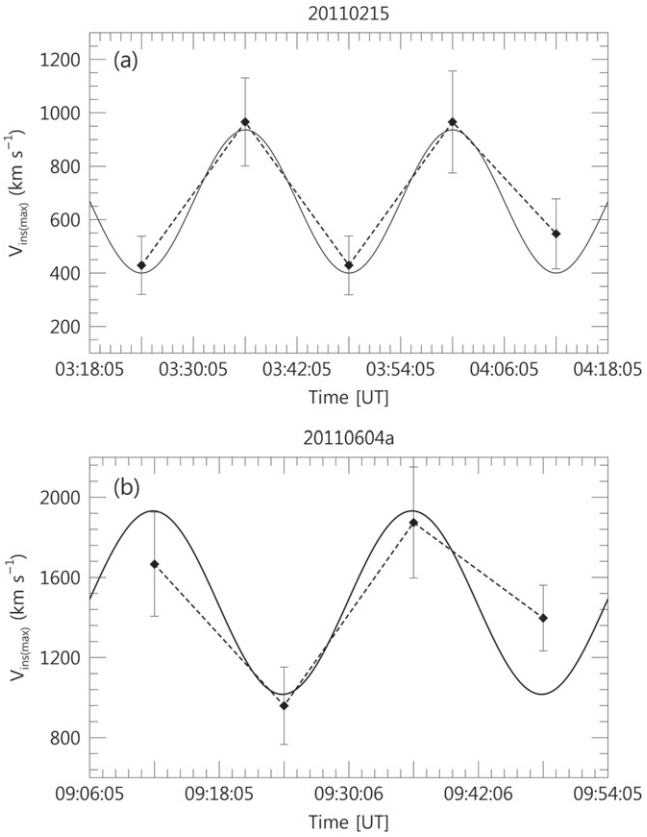

Figure 3. Two examples of HCME speed profiles $V_{ins(max)}$(dashed line) with maximum amplitudes and their comparison with harmonic functions (solid line). The error bars denote standard deviations.

same class of phenomena. At the coronagraph heights similar oscillations of the radial speed of CMEs have been detected by Krall et al. (2001) and Shanmugaraju et al. (2010). The HCME oscillations discussed here differ from them as we detect the oscillatory motion in the plane perpendicular to the direction of the CME motion. However, if this oscillation is observed from a line of sight almost, but not exactly perpendicular to the motion direction, it could result in the variation of the instantaneous radial speed seen by Krall et al. (2001) and Shanmugaraju et al. (2010).

We observe the oscillations in the radial direction on the plane of the sky. However, the phases of the radial oscillations along different radial rays are not in phase. This finding excludes the interpretation of the oscillations in terms of the sausage ($m = 0$) mode. The variations of the instantaneous speeds of HCME are found to have a clear structure in the azimuthal direction around the Sun, which corresponds to the "kink" ($m = 1$) and "fluting" ($m = 2$) oscillatory patterns. These oscillations could be caused by several physical mechanisms, including natural oscillations, driven oscillations, and self-oscillations.

One interpretation is connected with the natural oscillations of the plasmoid displaced from its equilibrium. In particular, estimations performed by Cargill et al. (1994) and Filippov et al. (2001) showed that a curved magnetic rope could perform oscillations with a period up to several tens of minutes. These models accounted for the restoring force caused by the perturbations of the magnetic field and also the aerodynamic drag force. These results would be consistent with the observed coincidence of the $m = 1$ oscillation polarization with the direction along the HCME position angle. In this case, the observed mode would be the second vertically polarized spatial harmonics ("swaying" oscillations, see Díaz et al. 2006) that displaces the CME rope in its plane. The oscillation period of this mode can be estimated as

$$P_{\rm swaying} \approx 3\pi D_{\rm rope}/C_A, \quad (1)$$

where C_A is the Alfvén speed, and $D_{\rm rope}$ is the major diameter of the rope, assuming it has a circular shape. The rope major diameter can be taken as the HCME diameter divided by 1.5 or so. The factor of 3 accounts for the increase in the period because of effects of curvature and twist (Cargill et al. 1994). From Equation (1) we obtained that for the HCME diameter $D = 20\,R_\odot$ and the observed periods $P = 30$ minutes, the Alfvén speed should be far too high, about 50,000 km s^{-1}. Even if we neglect the factor of 3, and hence the twist and curvature in Equation (1) the Alfvén speed is about 16,000 km s^{-1}, which is still unacceptably high. These values can be reduced by some integer value if we assume that the oscillation corresponds to a higher spatial harmonics along the rope axis, but there is no observational evidence for that. But, it is necessary to stress that the estimation (1) was obtained for a slender rope and it is not clear whether it is applicable to an HCME dynamics. Also, it is not clear whether this model can explain the observed correlation between the oscillation amplitudes and periods and the HCME speed. The established correlation of the oscillation amplitude and the HCME speed is indicative of the nonlinear nature of the observed phenomenon, that needs to be built-in the model.

Another possibility is connected with the typical zigzagging trajectory of an emerging body, connected with shedding of vortices (see Nakariakov et al. 2009; Gruszecki et al. 2010, for the discussion of this phenomenon in the coronal context). This mechanism belongs to the class of self-oscillations that appear because of the nonlinear conversion of DC energy (e.g., of the steady flow) in AC energy (e.g., the transverse oscillatory motion). In favor of this interpretation could also be the established dependence of the oscillation period and amplitude on the HCME speed. The period $P_{\rm vort}$ of the force experienced by a body due to shedding of vortices, which is perpendicular to the direction of the motion and hence produces the transverse oscillations, is determined by the flow speed U and the diameter D of the body, i.e., of the HCME plasmoid, as

$$P_{\rm vort} \approx ({\rm St})^{-1} D/U, \quad (2)$$

where St is a dimensionless coefficient known as the Strouhal number. For a bluff sphere, the Strouhal number ranges from 0.2 to 2, see, e.g., Figure 3 of Sakamoto & Haniu (1990). Making an order of magnitude estimations, we obtain that for the observed period of 30 minutes, the relative flow speed of 1000 km s^{-1} (that can be considered as the difference between the the observed projected speed of the HCME, $V_{\rm pro}$, and the solar wind speed), and the HCME diameter of $20\,R_\odot$, the Strouhal number should be about 7.7. This value may be acceptable as this estimation is very basic and does not take into account the effects of the magnetic field strength and its orientation, and the plasmoid boundary elasticity. Also, the expansion of the CME bubble should possibly lead to the

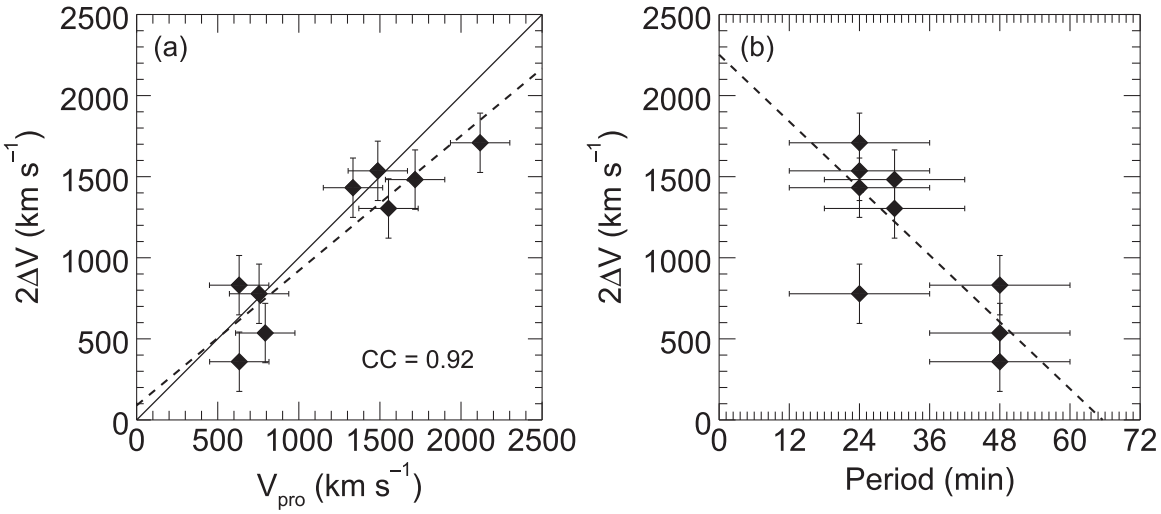

Figure 4. Correlation between (a) the observed maximum projected speed (V_{pro}) and the oscillation amplitude ($2\Delta V$) (b) the oscillation period and amplitude. The dashed line indicates linear fits to all data points and the solid line corresponds to that both quantities are perfectly consistent with each other. The error bars denote standard deviations.

change of the period with time. Perhaps this effect indeed takes place but cannot be seen in our data because of the lack of resolution. However, this interpretation should not be accepted until a detailed theoretical investigation of Alfvénic vortex shedding by an elastic expanding sphere in a magnetized plasma is carried out.

This work was supported by the BK21 plus program through the National Research Foundation (NRF) funded by the Ministry of Education of Korea, Basic Science Research Program through the NRF funded by the Ministry of Education (NRF-2013R1A1A2012763), and NRF of Korea grant funded by the Korean Government (NRF-2013M1A3A3A02042232). V.M.N. acknowledges the support from the European Research Council under the *SeismoSun* Research Project No. 321141, and STFC consolidated grant ST/L000733/1. The CME catalog is generated and maintained at the CDAW Data Center by NASA and The Catholic University of America in cooperation with the Naval Research Laboratory. *SOHO* is a project of international cooperation between the ESA and NASA.

REFERENCES

Bi, Y., Jiang, Y., Yang, J., et al. 2014, ApJ, 790, 100
Brueckner, G. E., Howard, R. A., Koomen, M. J., et al. 1995, SoPh, 162, 357
Cargill, P. J., Chen, J., & Garren, D. A. 1994, ApJ, 423, 854
De Moortel, I., & Nakariakov, V. M. 2012, RSPTA, 370, 3193
Díaz, A. J., Zaqarashvili, T., & Roberts, B. 2006, A&A, 455, 709
Filippov, B. P., Gopalswamy, N., & Lozhechkin, A. V. 2001, SoPh, 203, 119
Foullon, C., Verwichte, E., & Nakariakov, V. M. 2009, ApJ, 700, 1658
Foullon, C., Verwichte, E., Nakariakov, V. M., Nykyri, K., & Farrugia, C. J. 2011, ApJL, 729, L8
Gopalswamy, N., Lara, A., Lepping, R. P., et al. 2000, GeoRL, 27, 145
Gopalswamy, N., Lara, A., Yashiro, S., Kaiser, M. L., & Howard, R. A. 2001a, JGR, 106, 29207
Gopalswamy, N., Yashiro, S., Kaiser, M. L., Howard, R. A., & Bougeret, J.-L. 2001b, JGR, 106, 29219
Gosling, J. T. 1993, JGR, 98, 18937
Gosling, J. T., McComas, D. J., Phillips, J. L., & Bame, S. J. 1991, JGR, 96, 7831
Gruszecki, M., Nakariakov, V. M., van Doorsselaere, T., & Arber, T. D. 2010, PhRvL, 105, 055004
Hershaw, J., Foullon, C., Nakariakov, V. M., & Verwichte, E. 2011, A&A, 531, AA53
Krall, J., Chen, J., Duffin, R. T., Howard, R. A., & Thompson, B. J. 2001, ApJ, 562, 1045
Kim, S., Nakariakov, V. M., & Cho, K.-S. 2014, ApJL, 797, LL22
Lindsay, G. M., Luhmann, J. G., Russell, C. T., & Gosling, J. T. 1999, JGR, 104, 12515
Liu, W., & Ofman, L. 2014, SoPh, 289, 3233
Nakariakov, V. M., Aschwanden, M. J., & van Doorsselaere, T. 2009, A&A, 502, 661
Sakamoto, H., & Haniu, H. 1990, ATJFE, 112, 386
Shanmugaraju, A., moon, Y.-J., Cho, K.-S., et al. 2010, ApJ, 708, 450S
Tripathi, D., Isobe, H., & Jain, R. 2009, SSRv, 149, 283
Vršnak, B., & Žic, T. 2007, A&A, 472, 937
Vršnak, B., Ruždjak, D., Sudar, D., & Gopalswamy, N. 2004, A&A, 423, 717
Yashiro, S., Gopalswamy, N., Michalek, G., et al. 2004, JGRA, 109, 7105